Applied Catalysis B: Environmental 138–139 (2013) 122–127

Contents lists available at SciVerse ScienceDirect

Applied Catalysis B: Environmental

journal homepage: www.elsevier.com/locate/apcatb

The role of surface defect sites of titania nanoparticles in the photocatalysis: Aging and modification

Marija B. Radoičić[a], Ivana A. Janković[a], Vesna N. Despotović[b], Daniela V. Šojić[b], Tatjana D. Savić[a], Zoran V. Šaponjić[a], Biljana F. Abramović[b], Mirjana I. Čomor[a,*]

[a] Vinča Institute of Nuclear Sciences, University of Belgrade, P.O. Box 522, 11001 Belgrade, Serbia
[b] Department of Chemistry, Biochemistry and Environmental Protection, Faculty of Sciences, University of Novi Sad, Trg D. Obradovića 3, 21000 Novi Sad, Serbia

ARTICLE INFO

Article history:
Received 28 November 2012
Received in revised form 1 February 2013
Accepted 9 February 2013
Available online 27 February 2013

Keywords:
Colloidal nanoparticles
Surface modification
Titanium dioxide
Photocatalysis

ABSTRACT

A study of photocatalytic activity of bare as prepared, bare aged and dopamine surface modified colloidal TiO_2 nanoparticles was obtained following degradation reaction of herbicide RS-2-(4-chloro-o-tolyloxy)propionic acid under UV light irradiation. Results showed that the most active photocatalyst is bare aged TiO_2 and the least active are dopamine modified nanoparticles. Results are discussed in the light of surface structure of TiO_2 nanoparticles. The study of surface modification of TiO_2 nanoparticles (4.5 nm, TiO_2 NPs) with dopamine was also performed. The formation of inner-sphere charge-transfer complexes results in red shift of semiconductor absorption threshold (600 nm), compared to bare TiO_2 NPs (380 nm). Effective band gap energy of 3.2 eV for bare TiO_2 NPs is reduced to 2.1 eV for TiO_2/dopamine charge transfer complexes. The binding structure was investigated by UV-vis and FTIR spectroscopy. The obtained optimal geometry for binding of dopamine to surface Ti atoms was binuclear bidentate-bridging. From the Benesi–Hildebrand plot, stability constant of the order 10^3 M^{-1} has been determined.

1. Introduction

Nanoparticles (NPs) of TiO_2 have been intensively studied because of their potential unique applications in the photocatalytic clean up of water contaminated with hazardous industrial byproducts [1–4] or as a photoactive material in nanocrystalline solar cells [5–9]. Excitation of TiO_2 with light energy greater than its band gap (3.2 eV) generates electron–hole (e^-/h^+) pairs that can migrate to the particle surface and participate in reduction and oxidation processes at the surface. Although TiO_2 is very effective from an energetic point of view, it is relatively inefficient as a photocatalyst with respect to optimized photochemical systems such as natural photosynthesis. The main energy loss in all investigated particulate systems is due to the recombination of charges generated by illumination of semiconductor particles, which is manifested as the relatively low efficiency of long-lived charge separation. Also, the use of TiO_2 for photocatalytic applications driven by solar light is limited because of its wide band gap thus absorbing fewer than 5% of the available photons of the solar spectrum [3]. Therefore, the main focus of research for the application of titania assisted photocatalysis is to improve both the separation of charges and the TiO_2 response in the visible spectral region. These two goals can be achieved by, for example, dye sensitization of TiO_2 [5–10], using different composites based on TiO_2 [11,12], modification of TiO_2 [13,14] as well as doping with different elements [15–18].

The origin of the unique photocatalytic activities of TiO_2 NPs comparing to the bulk is found in larger surface area and the existence of surface sites with distorted coordination [19–22]. Owing to large curvature of TiO_2 particles in the nanosize regime, the surface must be reconstructed in such manner that distortion of the crystalline environment of surface Ti atoms occurs, forming coordinatively unsaturated Ti atoms (square-pyramidal i.e. pentacoordinated) [23]. These surface undercoordinated Ti (Ti_{surf}) atoms are very reactive and can act as traps for photogenerated charges [24]. Formation of these defect states go together with formation of oxygen vacancies [25,26]. Theoretical studies demonstrated that a high oxygen vacancy concentration can form electronic states vacancy band below conduction band and improve visible light absorption of titania [25]. Oxygen vacancies located at the surface of TiO_2 particles disappear quickly in the presence of oxygen and during aging [26]. Bulk oxygen vacancies, and the other types of defects, are much more stable.

It was reported, on a whole class of electron-donating enediol ligands [20,21,27], benzene derivatives [28] or mercaptocarboxylic acids [29] that binding to coordinatively unsaturated Ti atoms simultaneously adjusts their coordination to octahedral geometry at the surface of nanocrystallites and changes the electronic properties of TiO_2. In such hybrid structures localized orbitals

* Corresponding author. Tel.: +381 117408192; fax: +381 117408607.
E-mail address: mirjanac@vinca.rs (M.I. Čomor).

0926-3373/$ – see front matter © 2013 Elsevier B.V. All rights reserved.
http://dx.doi.org/10.1016/j.apcatb.2013.02.032

of surface-attached ligands, are electronically coupled with the delocalized electron levels from the conduction band of a TiO_2 semiconductor [30]. As a consequence, absorption of light by the charge-transfer (CT) complex yields to the excitation of electrons from the chelating ligand directly into the conduction band of TiO_2 NPs [27]. This results in a red shift of the semiconductor absorption compared to that of unmodified nanocrystallites and enables efficient harvesting of solar photons. Additionally, this type of electronic coupling yields to instantaneous separation of photogenerated charges into two phases, the holes localize on the donating organic modifier, and the electrons delocalize in the conduction band of TiO_2.

The main subject of this publication is evaluation of photocatalytic activity of colloidal TiO_2 particles in dependence of their surface structure (presence of Ti_{surf} defect sites). We used two approaches to modify TiO_2 NPs: aging and surface modification by enediol ligands. Surface modification was also used as a way to efficient charge separation and as a measure of the number of surface Ti defect states. As an extension of our previous work [31–33] herein, we also report study of surface modified TiO_2 NPs with dopamine (DAM). Photocatalytic activity of obtained titania nanoparticles was checked by degradation of herbicide, RS-2-(4-chloro-o-tolyloxy)propionic acid (MCPP), used since the mechanism of its degradation using different TiO_2 photocatalysts is well known [16,34–36]. MCPP is persistent herbicide and its photolysis can be neglected. Also it should be noted that it is used all over the world and very often found in drinking water [16].

2. Materials and Methods

All off the chemicals used were of the highest purity available. Dopamine hydrochloride was purchased from Sigma. The commercial herbicide MCPP (98% purity), obtained from the Chemical Factory "Župa" Kruševac, Serbia, was purified by conventional recrystallization from water–ethanol (1:1, v/v) solution, and its purity was checked by ^1H NMR spectrometry (Bruker AC-250). 85% H_3PO_4 was obtained from Lachema (Neratovice, Czech Republic). 99.8% acetonitrile (ACN) was a product of J.T. Baker.

The colloidal TiO_2 dispersions with the mean particle diameter of 4.5 nm were prepared from titanium(IV) chloride according to the procedure presented elsewhere [37]. Aged TiO_2 nanoparticles were prepared by refluxing fresh dispersions for 16 h at 60 °C.

A transmission electron microscope JEOL-JEM 2100 LaB6, operating at 200 kV, was used to determine the sizes of the TiO_2 nanoparticles.

XRD patterns were obtained by the standard powder diffraction methods with a Philips PW1830 X-ray powder diffractometer using a Cu K_a line.

Surface modification of fresh/aged TiO_2 resulting in the formation of a CT complex was achieved by the addition of surface-active ligand DAM up to concentrations required for full coverage ($[Ti_{surf}] = [TiO_2]12.5/D$ [38], where $[Ti_{surf}]$ is the molar concentration of surface Ti sites, $[TiO_2]$ is the molar concentration of TiO_2 in molecular units, and *D* is the diameter of the particle in angstroms). In order to avoid precipitation and/or "gelling" of the solution pH was adjusted to 2.0. For the determination of CT complex binding constants the absorption spectra were recorded at room temperature in cells with 1 cm optical path length using Thermo Scientific Evolution 600 UV/Vis spectrophotometer.

For the spectrophotometric determination of the complex composition continual variations method (Job's method [39]) was applied by mixing different volumes of equimolar solutions (2×10^{-3} M) of Ti_{surf} and DAM.

Infrared spectra were taken in attenuated total reflection (ATR) mode using a Nicolet 380 FTIR spectrometer equipped with a Smart Orbit^{TM} ATR attachment. Powder samples of surface modified TiO_2 nanoparticles were prepared by placing dispersions into the vacuum oven to get to complete dryness.

2.1. Photodegradation procedure

Photocatalytic degradation was carried out in a cell described previously [17]. Into 20 ml solution of MCPP (2.7×10^{-3} M) 2 ml of catalyst suspension was added. The mixture was then sonicated (50 Hz) in the dark for 15 min before irradiation, in order to make distribution of the catalyst particles uniform and attain adsorption equilibrium. The suspension thus obtained was thermostated at 25 ± 0.5 °C in a constant stream of O_2 (3.0 ml min^{-1}). Irradiation in the UV range was performed using a 125 W high-pressure mercury lamp (Philips, HPL-N, emission band in the UV region at 304, 314, 335 and 366 nm, with maximum emission at 366 nm). During the irradiation, the mixture was stirred at a constant speed. The lamp output was calculated to be ca. 8.8×10^{-9} Einstein ml^{-1} min^{-1} (potassium ferrioxalate actinometry). All experiments were carried out at a natural pH (~2.8).

2.2. Analytical procedure

For the kinetic studies of herbicide photodegradation by liquid chromatography–diode array detection (LC–DAD), aliquots (0.25 ml for MCPP to keep total volume change below 10%) of the reaction mixture were taken at the beginning of the experiment and at regular time intervals. Each aliquot was diluted to 10.00 ml with distilled water being acidified with 0.1% H_3PO_4 (pH ~2.3). The obtained suspensions were filtered through Millipore (Millex-GV, 0.22 μm) membrane filter. The absence of the MCPP adsorption on the filters was preliminarily checked.

An Agilent Technologies 1100 Series liquid chromatograph, equipped with a UV–vis diode array detection set at 228 nm (absorption maximum for MCPP), as well as at 230, 275 and 280 nm (for intermediates) and a Zorbax Eclypse XDB-C18 (150 mm × 4.6 mm i.d., particle size 5 μm, 25 °C) column were used to monitor the concentrations of MCPP and intermediates by injecting 20 μl samples. The mobile phase (flow rate 1 ml min^{-1}, pH = 2.68) was a mixture of ACN and water (1:1, v/v), the water being acidified with 0.1% H_3PO_4. Reproducibility of repeated runs was around 5−10%.

3. Results and discussion

3.1. Properties of bare TiO_2 NPs: fresh and aged

A typical TEM image and XRD spectrum of as-prepared and aged TiO_2 NPs are presented in Fig. 1a and b, respectively. TEM measurements (Fig. 1a) showed that TiO_2 NPs are nearly spherical and have diameters of about 4 nm. From Fig. 1b it can be seen that anatase crystalline structure is the only one present in both samples; peaks are assigned to corresponding crystalline planes, being much more pronounced after aging. Fresh TiO_2 NPs are almost amorphous. Prolonged thermal treatment (for 16 h at 60 °C) induced formation of well-defined crystalline domains with no change in absorption spectra. Because of small diffusion lengths in NP weakly bound defect lattice sites are easily healed upon aging. Hence bond lengths and bond angles in which photogenerated radicals can be trapped became ordered [40].

3.2. Properties of surface modified TiO_2 NPs

When TiO_2 particles are in the nanocrystalline regime, a large fraction of the atoms that constitute the nanoparticle is located at

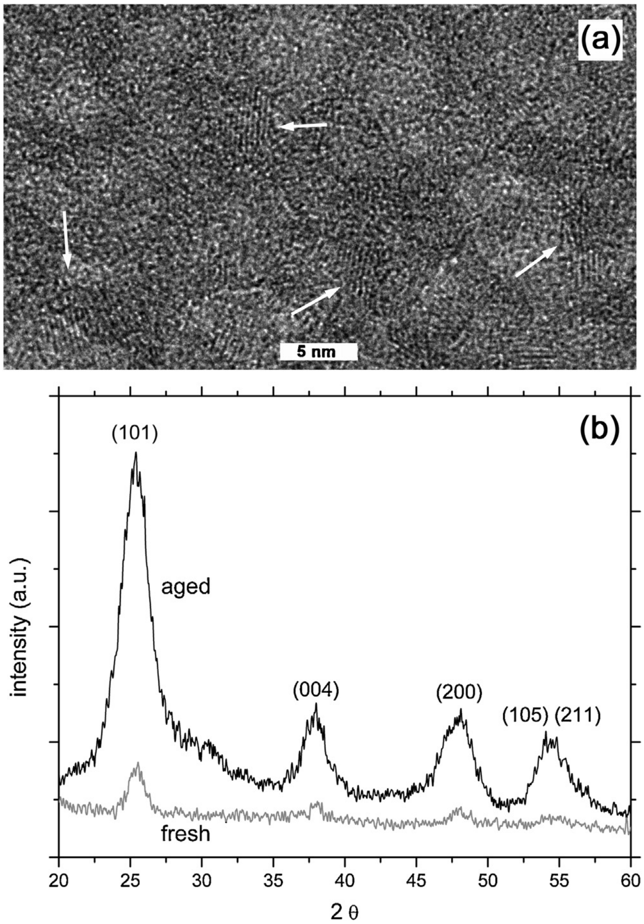

Fig. 1. (a) TEM of fresh TiO_2 NPs and (b) XRD patterns of TiO_2 NPs.

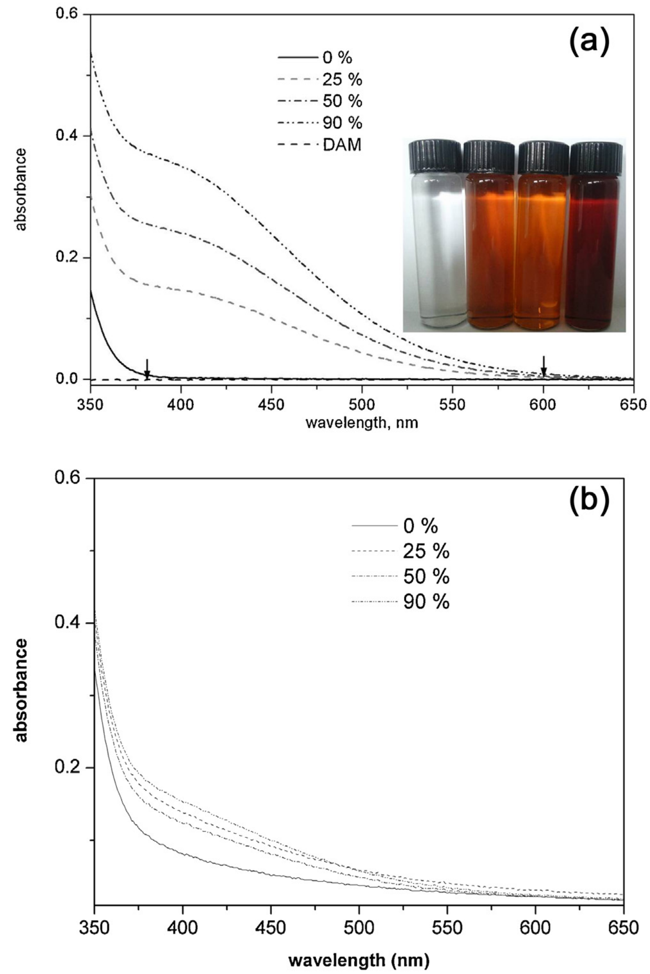

Fig. 2. Absorption spectra of bare and surface modified TiO_2 NPs: as prepared (a) and aged (b). $[TiO_2] = 3.6 \times 10^{-2}$ M, [DAM] = 10^{-3} M, pH = 2; surface coverages are presented in graphs.

the surface with significantly altered electrochemical properties. As the size of nanocrystalline TiO_2 becomes smaller than 20 nm the surface Ti atoms adjust their coordination environment from hexacoordinated (octahedral) to pentacoordinated (square pyramidal) [23] and these undercoordinated defect sites are the source of novel enhanced and selective reactivity of nanoparticles toward bidentate ligand binding. Dopamine, containing two adjacent phenolic groups, is found to undergo binding at the TiO_2 surface, inducing new hybrid properties of the surface-modified nanoparticle colloids [20,41–44].

These hybrid properties arise from the ligand-to-metal CT interaction coupled with electronic properties of the core of semiconductor nanoparticle. Consequently, the onset of absorption of these CT nanocrystallites is red shifted compared to unmodified TiO_2. The shift in the absorption edge in the modified semiconductor nanoparticles is attributed to the excitation of localized electrons from the surface modifier into the conduction band continuum states of the semiconductor particle [25]. The optical shift induced by TiO_2 surface modification with DAM is shown in Fig. 2a, with onsets of absorption depicted by arrows. For bare TiO_2, the wavelength of onset of absorption is 380 nm, corresponding to a band gap of 3.2 eV for anatase. Addition of dopamine on the TiO_2 surface shifts the onset of absorption to the visible range, due to the CT complex formation (absorption threshold 600 nm). Increasing the amount of dopamine increases absorbance at all wavelengths <600 nm but does not shift the onset of absorption [21]. Apart from the shift in the absorption edge, the optical properties of surface modified semiconductor nanoparticles, having a continuous rise of absorption toward higher energies, paralleled the absorption properties characteristic of the band structure in bare semiconductor nanoparticles. DAM modified TiO_2 NPs preserved their optical properties even after exposure to daylight, for months. Dispersions of TiO_2/DAM NPs used as photocatalysts in degradation of MCPP, were optically stable during exposure to UV–vis light (at least 3 h).

By deriving the corresponding onset wavelength from the absorption spectrum of DAM modified TiO_2 NPs, the effective band gap energy ($E(\text{eV}) = hc/\lambda = 1240/\lambda\,(\text{nm})$) was calculated to be 2.1 eV, matching well with the literature value [20,21].

The stoichiometric ratio between Ti_{surf} atoms and DAM in the CT complex was 2:1. This ratio was obtained by using Job's method of continuous variation [39] assuming that only one type of complex is present in solution (supplementary data: Fig. 1).

Stability constant K_b was determined from the absorbances of a series of solutions containing a fixed concentration of TiO_2 NPs (supplementary data: Fig. 2) and increasing concentrations of ligand. By plotting $1/A$ vs $1/[\text{DAM}]$ the straight line was obtained and from the ratio of the intercept and the slope, $K_b = 1400 \pm 100\ M^{-1}$ ($R = 0.998$) was determined. In the literature, K_b values of the same order of $10^3\ M^{-1}$ were also reported ($7900\ M^{-1}$, $4100\ M^{-1}$, $2500\ M^{-1}$) [20,41,42].

The way dopamine binds to TiO_2 surface was investigated by using ATR–FTIR spectroscopy. Since the infrared spectrum of dried TiO_2 has only the characteristic broad band in 3700–2000 cm^{-1} region [20], we were able to measure spectra of modified colloids in 1700–1000 cm^{-1} region where the characteristic bands of modifier

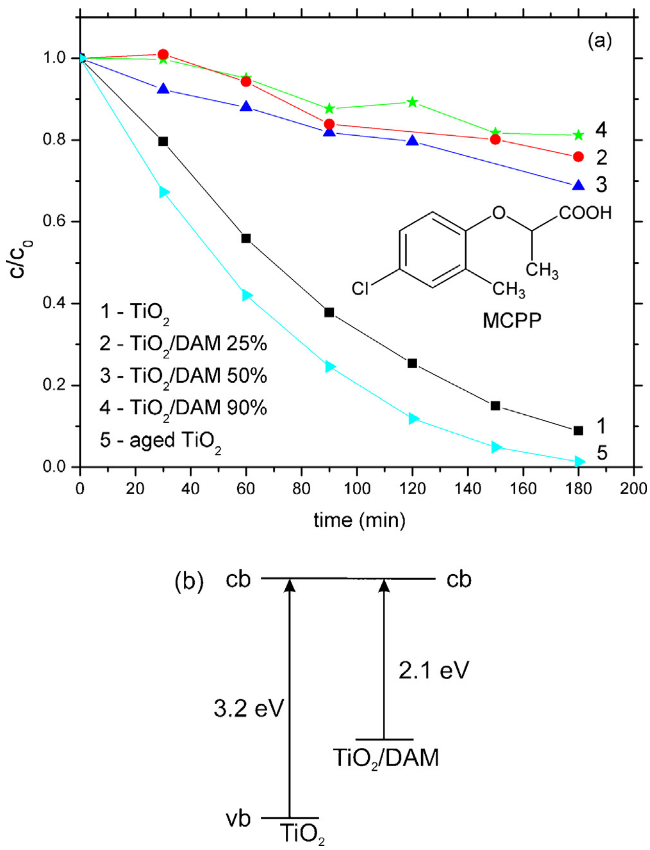

Fig. 3. (a) Kinetic curves of photocatalytic degradation of MCPP 1–4 fresh TiO_2 NPs, 5 aged TiO_2 under UV light and (b) energy level positions associated with surface modification of TiO_2 NPs obtained from the shift in absorption threshold.

exist (supplementary data: Fig. 3). Since according to Job's curve the molar ratio between Ti_{surf} atoms and DAM in the complex is 2:1, the CT complex formed is most likely bidentate binuclear (bridging) complex [45–47].

In Fig. 2b the optical shift induced by surface modification of aged TiO_2 NPs with DAM is shown. For all surface stoichiometric coverages (applied for fresh NPs) absorption intensities are significantly decreased suggesting that aging induced reorganizing of the NP surface, with less Ti_{surf} defect sites that can make charge-transfer complexes. Similar results were obtained for pyrogallol modified aged and as prepared TiO_2 NPs [32].

3.3. Photocatalytic degradation of MCPP

Although a numerous decomposition pathways of organic substrates in oxygenated aqueous solutions can be envisioned, the reactions of hydroxyl radicals, being strong oxidizing agents (standard redox potential 2.8 V), dominate, which is generally accepted [35]. A brief description of mechanism of photocatalytic degradation of MCPP using TiO_2 nanoparticles is given in Supplementary Data: Scheme 1.

Under UV light irradiation, as can be seen in Fig. 3a, MCPP can be decomposed with all applied photocatalysts. Although formation of TiO_2/DAM CT complex moved absorption onset of the nanoparticle dispersions into the visible spectral range (E_g = 2.1 eV), no significant photocatalytic activity using visible light irradiation was observed (results not presented). The best results however were obtained with bare fresh and bare aged TiO_2 NPs (Fig. 3a, curves 1 and 5). Both catalysts degrade herbicide MCPP when UV light is applied as expected [35], but aged NPs showed better activity. In oder to degrade 50% of initial MCPP concentration 50 min of irradiation was necessary when aged NPs were used and 70 min when as prepared NPs were used. Similar observations were made by Cropek et al. [40]. They employed EPR spectroscopy to explain processes associated with aging of TiO_2 NPs due to dependence between the nanocrystalline quality of the NPs and the width and the shape of EPR signals. It can be concluded that, when talking about bare nanodimensional TiO_2 photocatalysts, increase of the crystallinity of TiO_2 NPs and decrease in the number of surface Ti defects induce increase of their photocatalytic activity.

Table 1
Effect of type of catalyst on reaction rate constant of photocatalytic degradation of MCPP.

Type of catalyst	k' ($\times 10^3$ min^{-1})[a]	R[b]
Fresh bare TiO_2 NPs	11.6	0.995
TiO_2 NPs with 25% DAM	1.9	0.942
TiO_2 NPs with 50% DAM	1.9	0.989
TiO_2 NPs with 90% DAM	1.2	0.921
Aged bare TiO_2 NPs	17.9	0.989

[a] Reaction rate constant determined for the first 120 min of irradiation.
[b] Coefficients of correlation.

Modified TiO_2 NPs showed lower photocatalytic activity compared to bare NPs (Fig. 3a). It can be stressed that all modified photocatalysts (all % of surface coverage) had almost the same photocatalytic activity (Fig. 3a, Table 1). One of the possible reasons for such results may be the decreased availability of the surface for adsorption of MCPP on the modified TiO_2 nanoparticles. This fact might be the explanation for 50% or full coverage, but even 25% of coverage reduced photocatalytic activity. The other reason may be based on the formed TiO_2/DAM CT complex. Namely CT complex on the surface of TiO_2 NPs extracts photogenerated holes from TiO_2 NPs, as presented in Fig. 3b. Taking into account the potential of the extracted holes (Fig. 3b) which are not able to produce OH radicals capable for degradation of MCPP it seems that only electrons from TiO_2 conduction band participate in the degradation of MCPP. Just conduction band electrons react with surface adsorbed oxygen to produce superoxide radicals that subsequently induce degradation of herbicide in solution. As can be seen in Fig. 2, surface modification induced red shift of the absorption onset. As already stressed in literature [31], due to surface modification of TiO_2 NPs conduction band potential is constant while valence band potential of CT complex is moved to lower value and consequently holes extracted through CT complex are not capable to react with MCPP.

Using EPR spectroscopy, that provides an unambiguous identification of the species involved in the charge separation processes in TiO_2 nanoparticles and consequently in TiO_2/DAM CT complex upon photo-excitation, $(Ti^{3+})_{latt}$ and DAM^+ radical species were identified [48,49]. Based on narrowing of EPR signal attributed to DAM observed at g = 2.004 in TiO_2/DAM CT complex after deuteration (ring D_2 or 2,2 D_2) which indicated the existence of spin density on the pendant CH_2—CH_2—NH_2 side chain of DAM Rajh et al. [48] suggest delocalization of photogenerated holes to the pendant side chain. It is known that photogenerated charge pairs in this system could be separated over an extended distance (~2 nm) [50,51]. The destiny of DAM^+ radicals was not the subject of this study but we presume that they react with different transient species present in solution.

Bearing in mind that photocatalytic activity of all samples independently of DAM coverages (25%, 50% and 90%) are almost the same (Fig. 3a) we can say that DAM molecules are uniformly distributed on the surface of TiO_2 NPs. Otherwise photocatalytic activity of TiO_2/DAM 25% would be higher than 50% and 90%. It is possible that surface modification process affects the properties of the particle as a whole (the whole nanocrystallite, interior and surface) and even very low concentrations (small coverages) of TiO_2/DAM CT-complex are able to extract all photogenerated

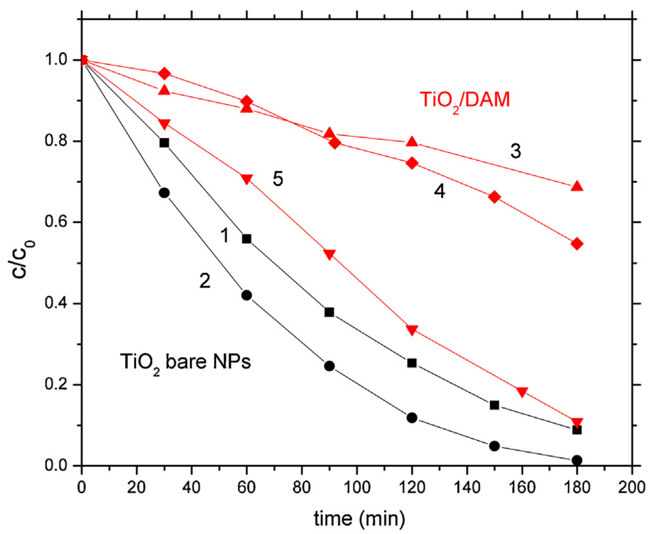

Fig. 4. Kinetic curves of photocatalytic degradation of MCPP using different TiO_2 NPs: 1 – fresh bare, 2 – aged 1, 3 – modified 1, 4 – aged 3, 5 – modified 2. DAM coverage was 50% in all modified samples.

holes and suppress their consumption through MCPP degradation process.

In Fig. 4 kinetic curves of photocatalytic degradation of MCPP using fresh (1), differently aged: bare (2) and modified (50%) (4), and differently modified, fresh (3) and aged (5) TiO_2 nanoparticles are presented. It can be seen that aging of modified TiO_2/DAM nanoparticles (4) didn't influence significantly their photocatalytic activity. Modification of aged TiO_2 nanoparticles (5) showed better photocatalytic activity compared to aged TiO_2/DAM nanoparticles (4) but worse compared to bare, fresh and aged, TiO_2 nanoparticles (1 and 2). Aging decreased the number of undercoordinated Ti defect sites on the surface of TiO_2 nanoparticles, but some still exist and make CT-complex with DAM (Fig. 2b).

Generally speaking our results showed that presence of undercoordinated Ti surface sites on TiO_2 NPs is not beneficial for photocatalytic degradation of herbicide MCPP. We obtained the best activity using bare aged NPs which have better crystallinity and reduced number of defect sites on the particle surface. It is well known that surface defect sites can influence photocatalytic activity by making intermediate complexes with substrates [17]. We checked this postulate by using surface modification process of TiO_2 NPs with DAM. As a result of modification, CT-complex was formed between Ti_{surf} sites and DAM. The stoichiometric ratio between Ti_{surf} atoms and DAM in the CT complex was 2:1. Stability constant K_b was determined; it was $1400 \pm 100\,M^{-1}$. Dopamine binds to TiO_2 NP surface through formation of bidentate binuclear (bridging) complex.

4. Conclusions

Photocatalytical degradation of herbicide MCPP was followed as model reaction for evaluation of photocatalytic activity of TiO_2 NPs based photocatalysts. Modified TiO_2 NPs showed reduced photocatalytic activity compared to bare TiO_2 NPs. Obtained results can be explained by reduced free TiO_2 surface after modification, at which MCPP can be adsorbed or inappropriate potential of holes extracted by CT complex, for direct oxidation of MCPP molecule. The best photocatalyst, among those which were the subject of this study, was found to be aged bare TiO_2 NPs. Binding of the dopamine molecules to undercoordinated surface Ti atoms (defect sites) results in formation of inner-sphere charge-transfer complex, observed by changes in the onset of absorption and effective band gap (2.1 eV). According to Job's method of continuous variation binding was bidentate binuclear (bridging, cateholate type). These complexes lead to restoration of the six-coordinated octahedral geometry of surface Ti atoms. Formation of CT-complex at a TiO_2 NP surface seems to affect particle as a whole, all photogenerated holes undergo extraction process from TiO_2 to TiO_2/DAM CT-complex and just photogenerated electrons can be used for degradation of MCPP.

Ackowledgements

The authors are grateful to Prof. S.P. Ahrenkiel from South Dakota School of Mines & Technology, USA for TEM measurements of titania nanoparticles. Financial support for this study was granted by Ministry of Education. Science and Technological Development of The Republic of Serbia, projects: 172056, 172042 and 45020.

Appendix A. Supplementary data

Supplementary data associated with this article can be found, in the online version, at http://dx.doi.org/10.1016/j.apcatb.2013.02.032.

References

[1] M.A. Fox, Topics in Current Chemistry 142 (1987) 71–99.
[2] H. Gerischer, A. Heller, Journal of Physical Chemistry 95 (1991) 5261–5267.
[3] Photocatalytic Purification and Treatment of Water and Air. In: Trace Met. EnViron. 1993, 3, Proceedings of the 1st International Conference on TiO_2 Photocatalytic Purification and Treatment of Water and Air, London, Ontario, Canada, November 8–13, 1992.
[4] D.F. Ollis, H. Al-Ekabi, in: N. Serpone, E. Pelizzetti (Eds.), Photocatalysis: Fundamentals and Applications, Wiley, NY, 1989.
[5] B. O'Regan, M. Grätzel, Nature 353 (1991) 737–740.
[6] C. Nasr, D. Liu, S. Hotchandani, P.V. Kamat, Journal of Physical Chemistry 100 (1996) 11054–11061.
[7] G.J. Meyer, Journal of Chemical Education 74 (1997) 652–656.
[8] R.J. Ellingson, J.B. Asbury, S. Ferrere, H.N. Ghosh, J.R. Sprague, T. Lian, A.J. Nozik, Zeitschrift fur Physikalische Chemie (Muenchen) 212 (1999) 77–84.
[9] N. Tetreault, M. Graetzel, Energy and Environmental Science 5 (2012) 8506–8516.
[10] X. Chen, C. Li, M. Graetzel, R. Kostecki, S.S. Mao, Chemical Society Reviews 41 (2012) 7909–7937.
[11] J. Ménesi, R. Kékesi, A. Oszkó, V. Zöllmer, T. Seemann, A. Richardt, I. Dékány, Catalysis Today 144 (2009) 160–165.
[12] Á. Veres, T. Rica, L. Janovák, M. Dömök, N. Buzás, V. Zöllmer, T. Seemann, A. Richardt, I. Dékány, Catalysis Today 181 (2012) 156–162.
[13] L. Korösi, Sz Papp I. Bertóti, I. Dékány, Chemistry of Materials 19 (2007) 4811–4819.
[14] L. Korösi, Sz Papp, J. Ménesi, E. Illés, V. Zöllmer, A. Richardt, I. Dékány, Colloids and Surfaces A 319 (2008) 136–142.
[15] R. Kun, S. Tarján, A. Oszkó, T. Seemann, V. Zöllmer, M. Busse, I. Dékány, Journal of Solid State Chemistry 182 (2009) 3076–3084.
[16] D.V. Šojić, V.N. Despotović, N.D. Abazović, M.I. Čomor, B.F. Abramović, Journal of Hazardous materials 179 (2010) 49–56.
[17] B.F. Abramović, D.V. Šojić, V.B. Anderluh, N.D. Abazović, M.I. Čomor, Desalination 244 (2009) 293–302.
[18] X. Chen, S.S. Mao, Chemical Reviews 107 (2007) 2891–2959.
[19] Z.V. Šaponjić, N.M. Dimitrijević, D.M. Tiede, J.A. Goshe, X. Zuo, L.X. Chen, A.S. Barnard, P. Zapol, L. Curtiss, T. Rajh, Advanced Materials 17 (2005) 965–971.
[20] T. Rajh, L.X. Chen, K. Lukas, T. Liu, M.C. Thurnauer, D.M. Tiede, Journal of Physical Chemistry B 106 (2002) 10543–10552.
[21] L. de la Garza, Z.V. Šaponjić, N.M. Dimitrijević, M.C. Thurnauer, T. Rajh, Journal of Physical Chemistry B 110 (2006) 680–686.
[22] W. Macyk, K. Szaciłowski, G. Stochel, M. Buchalska, J. Kuncewicz, P. Łabuz, Coordination Chemistry Reviews 254 (2010) 2687–2701.
[23] L.X. Chen, T. Rajh, W. Jäger, J.M. Nedeljković, M.C. Thurnauer, Journal of Synchrotron Radiation 6 (1999) 445–447.
[24] N.M. Dimitrijević, Z.V. Šaponjić, D.M. Bartels, M.C. Thurnauer, D.M. Tiede, T. Rajh, Journal of Physical Chemistry B 107 (2003) 7368–7375.
[25] N.D. Abazović, M.I. Čomor, M.D. Dramićanin, D.J. Jovanović, S.P. Ahrenkiel, J.M. Nedeljković, Journal of Physical Chemistry B 110 (2006) 25366–25370.
[26] W. Wang, C. Lu, Y. Ni, J. Song, M. Su, Z. Xu, Catalysis Communications 22 (2012) 19–23.
[27] T. Rajh, J.M. Nedeljković, L.X. Chen, O. Poluektov, M.C. Thurnauer, Journal of Physical Chemistry B 103 (1999) 3515–3519.
[28] J. Moser, S. Punchihewa, P.P. Infelta, M. Graetzel, Langmuir 7 (1991) 3012–3018.

[29] T. Rajh, D.M. Tiede, M.C. Thurnauer, Journal of Non-Crystalline Solids 205–207 (1996) 815–820.
[30] P. Persson, R. Bergström, S. Lunell, Journal of Physical Chemistry B 104 (2000) 10348–10351.
[31] I.A. Janković, Z.V. Šaponjić, M.I. Čomor, J.M. Nedeljković, Journal of Physical Chemistry C 113 (2009) 12645–12652.
[32] I.A. Janković, Z.V. Šaponjić, E.S. Džunuzović, J.M. Nedeljković, Nanoscale Research Letters 5 (2010) 81–88.
[33] T.D. Savić, I.A. Janković, Z.V. Šaponjić, M.I. Čomor, D.Ž. Veljković, S.D. Zarić, J.M. Nedeljković, Nanoscale 4 (2012) 1612–1619.
[34] A. Topalov, M. Kosanić, D. Molnár-Gábor, B. Abramović, Water Research 34 (2000) 1473–1478.
[35] A. Topalov, D.V. Šojić, D. Molnár-Gábor, B. Abramović, M.I. Čomor, Applied Catalysis B: Environmental 54 (2004) 125–133.
[36] B. Abramović, D.V. Šojić, V. Anderluh, Acta Chimica Slovenica 54 (2007) 558–564.
[37] T. Rajh, A.E. Ostafin, O.I. Micic, D.M. Tiede, M.C. Thurnauer, Journal of Physical Chemistry 100 (1996) 4538–4545.
[38] L.X. Chen, T. Rajh, Z. Wang, M.C. Thurnauer, Journal of Physical Chemistry B 101 (1997) 10688–10697.
[39] W.C. Vosburgh, G.R. Copper, Journal of the American Chemical Society 63 (1941) 437–442.
[40] D. Cropek, P.A. Kemme, O.V. Makarova, L.X. Chen, T. Rajh, Journal of Physical Chemistry C 112 (2008) 8311–8318.
[41] C. Creutz, M.H. Chou, Inorganic Chemistry 47 (2008) 3509–3514.
[42] S. Varaganti, G. Ramakrishna, Journal of Physical Chemistry C 114 (2010) 13917–13925.
[43] M. Vega-Arroyo, P.R. LeBreton, T. Rajh, P. Zapol, L.A. Curtiss, Chemical Physics Letters 406 (2005) 306–311.
[44] K. Syres, A. Thomas, F. Bondino, M. Malvestuto, M. Gratzel, Langmuir 26 (2010) 14548–14555.
[45] W.B. Person, Journal of the American Chemical Society 87 (1965) 167–170.
[46] S.C. Li, J.G. Wang, P. Jacobson, X.Q. Gong, A. Selloni, U. Diebold, Journal of the American Chemical Society 131 (2009) 980–984.
[47] K.L. Syres, A.G. Thomas, W.R. Flavell, B.F. Spencer, F. Bondino, M. Malvestuto, A. Preobrajenski, M. Grätzel, Journal of Physical Chemistry C 116 (2012) 23515–23525.
[48] T. Rajh, Z. Šaponjić, J. Liu, N.M. Dimitrijević, N.F. Scherer, M. Vega-Arroyo, P. Zapol, L.A. Curtiss, M.C. Thurnauer, Nano Letters 4 (2004) 1017–1023.
[49] T. Rajh, O. Poluektov, A.A. Dubinski, G. Wiederrecht, M.C. Thurnauer, A.D. Trifunac, Chemical Physics Letters 344 (2001) 31–39.
[50] N.M. Dimitrijević, Z.V. Šaponjić, B.M. Rabatic, T. Rajh, Journal of the American Chemical Society 127 (2005) 1344–1345.
[51] M. Vega-Arroyo, P.R. LeBreton, P. Zapol, L.A. Curtiss, T. Rajh, Chemical Physics 339 (2007) 164–172.